

# Concatenated toolkit for quantum optimal control wave-function propagation

Michael Hsieh and Herschel Rabitz

*Department of Chemistry, Princeton University, Princeton, New Jersey 08544, USA*

(Received 7 December 2007; published 17 March 2008)

Numerical propagation of the Schrödinger equation is the bottleneck in many quantum optimal control computations. For a quantum system of  $N$  states with an electric-field-dipole interaction, the use of a propagation toolkit introduced in a prior work yields an  $O(N)$  reduction in floating-point operations per wave function propagation. A concatenation scheme for the toolkit method is introduced, and a scaling analysis shows a significant additional reduction in computational cost. The method exploits the fact that the same sequences of discretized control field values are often repeated many times in a control simulation. The concatenated toolkit is benchmarked against the standard toolkit in a numerical simulation.

DOI: [10.1103/PhysRevE.77.037701](https://doi.org/10.1103/PhysRevE.77.037701)

PACS number(s): 02.70.-c, 31.15.xv

## I. INTRODUCTION

Quantum optimal control theory [1] has been implemented successfully across a variety of physical models [2–16]. In such studies, a common bottleneck is the propagation of the wave function (as well as the density matrix or time evolution operator, depending on the objective) through the solution of Schrödinger’s equation. A propagation toolkit technique was proposed as a means of reducing this computational cost [17]. The toolkit concept is most naturally applied to quantum systems expressed in terms of a finite set of basis states, but it has also found utility in spatial wave-packet propagation [18]. In the present work we introduce a generalization of the original toolkit method [17] which yields further savings.

Consider a quantum system of  $N$  states whose dynamics are determined by Schrödinger’s equation

$$i\frac{\partial}{\partial t}|\psi(t)\rangle = [H_0 - \mu\varepsilon(t)]|\psi(t)\rangle, \quad (1)$$

where  $H_0$  is the free Hamiltonian,  $\mu$  is the dipole, and  $\varepsilon(t)$  is the control field. Here we adopt units of  $\hbar=1$ . The conventional approach to propagating the wave function entails discretizing time into  $L$  points  $\{t_1, \dots, t_L\}$ , taken as equally spaced by  $\Delta t$  for simplicity, and computing the product

$$|\psi(t_L)\rangle = \prod_{s=1}^L \exp[-iH(t_s)\Delta t]|\psi(t_1)\rangle, \quad (2)$$

where the Hamiltonian  $H(t_s)=H_0-\mu\varepsilon(t_s)$  is exponentiated anew at each time point. In typical optimal control applications, Schrödinger’s equation is solved repeatedly (commonly  $\sim 10^2-10^4$  times) for a sequence of control fields. This process incurs a recurrent computational cost scaling as  $O(LN^3)$  floating-point operations (FLOPs) for each full propagation to time  $t_L$ . In special cases the number of FLOPs may be less, but in general circumstances maintaining the highest accuracy will exhibit a scaling cubic in  $N$ .

An alternative approach [17] of propagation via the toolkit entails discretization of the control field amplitudes into a mesh of  $2D+1$  values  $\{\varepsilon_r\}$  indexed by  $r \in \{-D, -D+1, \dots, 0, \dots, D-1, D\}$  and ordered  $\varepsilon_r < \varepsilon_{r+1}$ . The maximum (minimum) discretized value of the field is  $\varepsilon_D$  ( $\varepsilon_{-D}$ ), along

with  $\varepsilon_0=0$ , and the mesh spacing is  $\varepsilon_{r+1}-\varepsilon_r=\Delta\varepsilon$  for all  $r$ ; equal spacing  $\Delta\varepsilon$  is not required, but it is convenient here to illustrate the basic toolkit concept. For each amplitude  $\varepsilon_r$  the corresponding short-time propagator  $\omega(r) \equiv \exp[-i(H_0 - \mu\varepsilon_r)\Delta t]$  is computed and the collection of all  $2D+1$  propagators  $\{\omega(r)\}$  is stored as the propagation toolkit. Figure 1 shows the result of applying three toolkits with  $D=10, 20$ , and  $50$  for an electric field bounded by the dynamic range  $-1 \leq \varepsilon(t) \leq 1$  and defined over a time interval discretized into  $L=300$  time points (arbitrary units are used and later for all numerical examples). As a practical guideline, the parameters  $D$  and  $L$  should be chosen such that the field does not jump more than two or three spacings of  $\Delta\varepsilon$  per time step  $\Delta t$ . If greater jumps are required, it is likely that either the amplitude or the time mesh is not well specified, possibly compromising the accuracy of the computation.

The computation of the propagators comprising the toolkit introduces a one-time overhead cost scaling as  $O((2D+1)N^3)$ . However, each subsequent solution of the Schrödinger equation

$$|\psi(t_L)\rangle = \prod_{\ell=1}^L \omega(r_\ell)|\psi(t_1)\rangle \quad (3)$$

for a new trial field now requires only matrix-vector multiplications of toolkit propagators with the initial wave function incurring a cost scaling as  $O(LN^2)$ . Here it is understood that each local propagator  $\omega(r_\ell)$  is some suitable member of the toolkit  $\{\omega(r)\}$  with  $r_\ell$  identified with a particular value of  $r$ . Since generally  $D \ll L$  and many propagations are required in most practical optimal control calculations, the one-time cost of computing the toolkit is amply compensated for by the subsequent  $O(N)$  savings accrued during each wave-function propagation.

The motivation for the foregoing *standard toolkit* concept arises from the observation that certain amplitude values of the electric field are repeated several times during the propagation, which is evident in Fig. 1 by taking a cut at any value of  $\varepsilon_r$ . This observation can be generalized by realizing that certain sequences of amplitude values are often repeated as well. This motivates the concept of the *concatenated toolkit*, discussed in the next section.

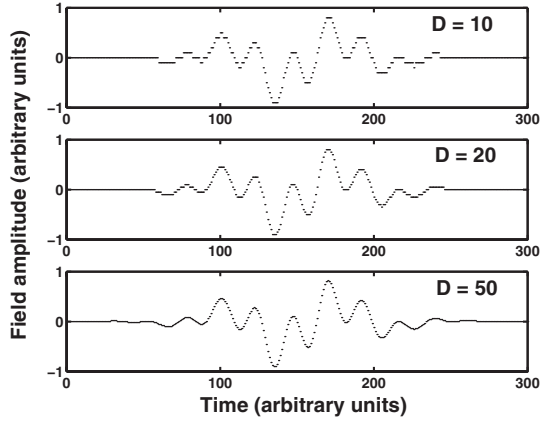


FIG. 1. An electric field bounded over the dynamic range  $\varepsilon_{-D} = -1$  and  $\varepsilon_D = 1$  with a 300-point time mesh (arbitrary units of amplitude and time are used) is discretized with three amplitude meshes  $D=10, 20, 50$ . Generally, larger  $D$  values correspond to smoother representations of the control field.

## II. CONCATENATED TOOLKIT

The propagators from the standard toolkit can be concatenated in a simple manner to further reduce the computational cost per propagation. The operations involve (i) precalculating  $C$ -length products of the standard toolkit propagators (which are denoted as *codons*), (ii) saving the codons into memory, and (iii) propagating the wave function with codons in lieu of the standard toolkit propagators. Beyond the overhead of calculating the codons, this concatenated toolkit procedure reduces the computational cost per propagation by a factor of  $\frac{1}{C}$ .

The standard toolkit is composed of a set of  $2D+1$  propagators  $\{\omega(r)\}$ . The concatenated toolkit is composed of all  $C$ -length products of propagators  $\omega(r)$  of the form

$$\begin{aligned} \Omega[r^{(C)}, \dots, r^{(j)}, \dots, r^{(2)}, r^{(1)}] \\ \equiv \omega(r^{(C)}) \cdots \omega(r^{(j)}) \cdots \omega(r^{(2)})\omega(r^{(1)}), \end{aligned} \quad (4)$$

satisfying the condition

$$|r^{(j+1)} - r^{(j)}| \leq M, \quad C > j \geq 1 \quad (5)$$

for each  $r^{(j)} \in \{-D, -D+1, \dots, 0, \dots, D-1, D\}$ . The condition (5) restricts “jumps” in the field value from one time step to the next to at most  $M\Delta\varepsilon$ . For a well-specified amplitude and time mesh,  $M=3$  is usually sufficient.

In Fig. 2, all possible codons originating from a given field value  $\varepsilon_k$  are illustrated for  $C=3$  and  $M=1$ . Proceeding from left to right, all possible paths leading from the node at time  $t$  to the nodes at time  $t+2\Delta t$  represent products to be computed and stored as codons. As an example, the path indicated by solid lines corresponds to the product  $\Omega[k-1, k-1, k] = \omega(k-1)\omega(k-1)\omega(k)$ . By direct counting of all paths, it is evident that there are  $(2M+1)^{C-1}$  codons originating from each  $\varepsilon_k$  (with the exception of the field values  $\varepsilon_{-D+\ell}$  and  $\varepsilon_{D-\ell}$  where  $\ell \leq CM$ , for which codons corresponding to paths leading to field values beyond the dynamic range  $[\varepsilon_{-D}, \varepsilon_D]$  are disregarded). Since there are  $2D+1$  values for  $\varepsilon_k$  in the field amplitude mesh,  $2D+1$  distinct collections of

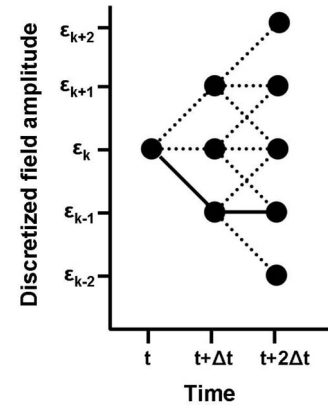


FIG. 2. A concatenated toolkit is composed of all  $C$ -length products of standard toolkit propagators satisfying the maximum jump rule in Eq. (5). In the present case,  $M=1$  and  $C=3$ . The  $\varepsilon_k$  amplitude value at time  $t$  is represented by a node, and all left-to-right paths leading from that node to the five nodes at time  $t+2\Delta t$  symbolize a product of toolkit propagators to be computed and stored as codons. As an illustration, the path defined by the solid lines is the codon  $\Omega[k-1, k-1, k] = \omega(k-1)\omega(k-1)\omega(k)$ .

codons originating from each  $\varepsilon_k$  must be computed and stored, as illustrated in Fig. 2. The one-time overhead cost of generating the concatenated toolkit scales as

$$O((2D+1)(2M+1)^{C-1}N^3), \quad (6)$$

where it is assumed that the standard toolkit has already been calculated.

Propagating a wave function with the concatenated toolkit involves (i) converting the actual field amplitude values to the discretized values permitted by the amplitude mesh, (ii) matching sequences of these values to the appropriate codons stored in memory, and (iii) performing matrix-vector multiplications of the evolving wave function with the matrices  $\Omega_\ell[r^{(C)}, \dots, r^{(j)}, \dots, r^{(2)}, r^{(1)}]$  representing the codons:

$$|\psi(t_L)\rangle = \prod_{\ell=1}^{L/C} \Omega_\ell[r^{(C)}, \dots, r^{(j)}, \dots, r^{(2)}, r^{(1)}] |\psi(t_1)\rangle. \quad (7)$$

Here it is understood that the particular codon sequence  $r^{(C)}, \dots, r^{(j)}, \dots, r^{(2)}, r^{(1)}$ ,  $C > j \geq 1$ , depends on the index  $\ell$ . The computational cost of a single wave-function propagation associated with the concatenated toolkit scales as  $O(\frac{L}{C}N^2)$ .

## III. COMPARISON OF COMPUTATIONAL COSTS

The construction of the concatenated toolkit introduces an added overhead computational cost beyond constructing the standard toolkit. However, application of the concatenated toolkit can yield a substantial savings in the computational cost of each solution of the Schrödinger equation. Furthermore, the accuracy of the concatenated toolkit is exactly the same as that for the standard toolkit, which is close to ordinary propagation assuming that the number  $2D+1$  of amplitude values is sufficiently large.

TABLE I. The ratios of the CPU time per propagation with the concatenated toolkit ( $\tau_c$ ) to that with the standard toolkit ( $\tau_s$ ) computed and averaged over 1000 propagations, for  $N=4$ ,  $D=50$ , and  $M=3$ . The averaged savings ratios  $\langle \frac{\tau_c}{\tau_s} \rangle$  correspond closely to the theoretically expected savings ratio  $\frac{1}{C}$  with the small discrepancy attributable to the per-propagation overhead cost of matching sequences of the discretized field values to their corresponding codons.

Codon length $C$	2	3	4	5	6
Observed $\langle \frac{\tau_c}{\tau_s} \rangle$	0.520	0.349	0.263	0.210	0.174
Theoretical savings ratio	0.500	0.333	0.250	0.200	0.167

To make a direct comparison, 1000 electric fields were randomly generated over a time interval  $[0,1]$  and discretized over  $L=300$  mesh points. The dynamic range of the fields was bounded over  $-1 \leq \varepsilon(t) \leq 1$ , and discretized with amplitude mesh parameter  $D=50$  (i.e., 101 mesh points). The free Hamiltonians  $H_0$  and dipoles  $\mu$  are randomly chosen for each field, where  $N=4$ . The ratios of the CPU time per propagation used by the concatenated toolkit ( $\tau_c$ ) to that for the standard toolkit ( $\tau_s$ ) are calculated for each of the 1000 fields for  $C=2, 3, 4, 5$ , and 6. The observed savings ratios  $\langle \frac{\tau_c}{\tau_s} \rangle$  shown in Table I, averaged over the 1000 fields, correspond closely with  $\frac{1}{C}$ . In general, increasing  $C$  reduces the computational cost per propagation. However, since the overhead cost of generating the concatenated toolkit scales exponentially with  $C$ , large values of  $C$  are impractical. In the next section, a guideline for choosing the value of  $C$  is developed based on the simple criterion that the savings introduced by the concatenation should exceed the additional overhead costs.

#### IV. SELECTION OF THE CODON LENGTH

Generally, a single quantum control computation seeking an optimal field requires multiple propagations of the Schrödinger equation. Letting  $J$  denote the number of propagations required in a given computation, the savings introduced by the use of the concatenated toolkit is  $JLN^2 - J\frac{L}{C}N^2$ . An approach to specifying an upper bound on  $C$  is to determine the value at which the total savings from all propagations in a computation exceeds the computational overhead given in Eq. (6), or

$$JLN^2 - J\frac{L}{C}N^2 \geq (2D+1)(2M+1)^{C-1}N^3. \quad (8)$$

Taking logarithms, this simplifies to

$$\ln\left(\frac{JL}{N(2D+1)}\right) \geq (C-1)\ln(2M+1) - \ln\left(1 - \frac{1}{C}\right). \quad (9)$$

Noting that  $-0.69 < \ln(1 - \frac{1}{C}) < 0$  for  $C \geq 2$ , it follows that

$$\frac{\ln\left(\frac{JL}{N(2D+1)}\right)}{\ln(2M+1)} + 1 > C. \quad (10)$$

Equation (10) provides a useful practical upper bound which can be readily calculated in advance of any application of the

concatenated toolkit with the available parameters  $J, L, D, N$ , and  $M$ . The parameter  $N$  is fixed by the physical system, and  $D, L$ , and  $M$  are fixed by requirements of accuracy, so the practical factor for determining the upper bound is  $J$ . For example, in the case of  $N=20, L=1000, D=50$ , and  $M=3$ , a codon length of up to 3 is justified for  $J=10^2$ , up to 4 for  $J=10^3$ , and up to 5 for  $J=10^4$ . Practically, it is preferable to choose a codon length beneath the actual upper bound, as the exponential increase in overhead for each further increase in  $C$  can be excessively expensive, even if justified by the bounding analysis.

#### V. FURTHER APPLICATIONS

Beyond wave-function propagation, there are classes of quantum control computations which involve the time propagation of a density matrix satisfying the equation  $i\frac{\partial}{\partial t}\rho(t) = [H(t), \rho(t)]$ , where the time evolution is given by  $\rho(t_L) = U(t_L, t_1)\rho(t_1)U^\dagger(t_L, t_1)$ . If  $\rho(t_1)$  describes a statistical mixture with no nonzero off-diagonal matrix elements, the FLOP cost of computing  $\rho(t_L)$  with the standard toolkit scales as  $O(LN^2)$  as only matrix-vector multiplications are required. The magnitude of the savings here, upon using the concatenated instead of the standard toolkit, is  $\sim \frac{1}{C}$ . However, if  $\rho(t_1)$  describes a coherent ensemble with nonzero off-diagonal terms, matrix-matrix multiplications are required and the FLOP cost for the standard toolkit scales as  $O(LN^3)$ . In this case the savings ratio is still  $\frac{1}{C}$  over the standard toolkit, but the significance of the savings is greater in absolute terms. The same savings are obtained for computing the propagator itself  $U(t_L, t_1)$  as well.

The savings from applying the standard toolkit method have been verified in practical calculations [19–24]. A code for a concatenated toolkit requires simple additional logic steps for computing the codons, and the overhead is generally small. The concatenated toolkit provides a simple, easily implementable refinement to the standard application of toolkit-based propagation for quantum control computations.

#### ACKNOWLEDGMENTS

Support from the NSF and USARO is acknowledged. M.H. acknowledges the support of the NDSEG.

- [1] S. Shi and H. Rabitz, *Chem. Phys.* **139**, 185 (1989).
- [2] C. Meier and M. Heitz, *J. Chem. Phys.* **123**, 044504 (2005).
- [3] I. Serban, J. Werschnik, and E. K. U. Gross, *Phys. Rev. A* **71**, 053810 (2005).
- [4] M. Sukharev and T. Seideman, *Phys. Rev. Lett.* **93**, 093004 (2004).
- [5] C. M. Tesch and R. de Vivie-Riedle, *J. Chem. Phys.* **121**, 12158 (2004).
- [6] E. Luc-Koenig, R. Kosloff, F. Masnou-Seeuws, and M. Vatasescu, *Phys. Rev. A* **70**, 033414 (2004).
- [7] D. Babikov, *J. Chem. Phys.* **121**, 7577 (2004).
- [8] B. Lan, I. Vrabel, and W. Jakubetz, *J. Chem. Phys.* **121**, 10401 (2004).
- [9] J. P. Palao and R. Kosloff, *Phys. Rev. A* **68**, 062308 (2003).
- [10] D. Geppert, A. Hoffman, and R. de Vivie-Riedle, *J. Chem. Phys.* **119**, 5901 (2003).
- [11] T. Hornung, S. Gordienko, R. de Vivie-Riedle, and B. Verhaar, *Phys. Rev. A* **66**, 043607 (2002).
- [12] J. P. Palao and R. Kosloff, *Phys. Rev. Lett.* **89**, 188301 (2002).
- [13] T. Mançal, U. Kleinekathöfer, and V. May, *J. Chem. Phys.* **117**, 636 (2002).
- [14] T. Hornung, M. Motzkus, and R. de Vivie-Riedle, *J. Chem. Phys.* **115**, 3105 (2001).
- [15] Y. Ohtsuki, H. Kono, and Y. Fujimura, *J. Chem. Phys.* **109**, 9318 (1998).
- [16] R. Kosloff, S. A. Rice, P. Gaspard, S. Tersigni, and D. Tannor, *Chem. Phys.* **139**, 201 (1989).
- [17] F. Yip, D. Mazziotti, and H. Rabitz, *J. Chem. Phys.* **118**, 8168 (2003).
- [18] Y. Maday and G. Turinici, *J. Quantum Chem.* **93**, 223 (2003).
- [19] Z. Shen, M. Hsieh, and H. Rabitz, *J. Chem. Phys.* **124**, 204106 (2006).
- [20] A. Rothman, T. S. Ho, and H. Rabitz, *Phys. Rev. A* **72**, 023416 (2005).
- [21] G. Balint-Kurti *et al.*, *J. Chem. Phys.* **122**, 084110 (2005).
- [22] I. Sola and H. Rabitz, *J. Chem. Phys.* **120**, 9009 (2004).
- [23] D. A. Mazziotti, *Phys. Rev. A* **69**, 012507 (2004).
- [24] X. S. Li, S. Smith, A. Markevitch, D. Romanov, R. Levis, and H. Schlegel, *Phys. Chem. Chem. Phys.* **7**, 233 (2005).